ISSN 1330-3651 (Print), ISSN 1848-6339(Online)
Received: 13 June 2025; Accepted: 10 August 2025

https://doi.org/10.17559/TV-20250613002744
Original scientific paper

High-Efficiency X-Band Rectenna Design for Wireless Power Transmission in Drone Applications

V.GANESH*, H.MANGALAM

Abstract: Wireless Power Transmission (WPT) has emerged as a promising technology for applications such as solar power satellites and high-altitude platforms, including UAVs, drones, and aircraft, with ongoing advancements in microwave-based systems enhancing efficiency and performance. Drones require lightweight, compact antennas for effective WPT, making microstrip patch arrays on low-density substrates an ideal choice. To overcome the limited gain of small antennas, a quasi Yagi-Uda design is implemented, offering a balanced solution with moderate gain, wide beamwidth, and compact size. The antenna is fabricated on a 10 mil Rogers RT/duroid 5880 substrate, known for its low dielectric constant and ultra-low loss tangent, making it suitable for X-band drone applications. The design includes a driven dipole, director, reflector, and additional directors to enhance gain, achieving beamwidths of 42° in the E-plane and 56° in the H-plane with a gain of 8.75 dBi. On the rectifier side, efficient power conversion is critical, especially at higher input levels where PCE typically decreases. A two-section quarter-wave transformer, low-pass filter, and DC pass filter are integrated to improve impedance matching and bandwidth. The proposed rectifier achieves peak PCE values between 53% and 57% for input powers of 20-50 mW, with over 50% PCE across a 0.75 GHz bandwidth and more than 40% across 1.75 GHz. The system's effectiveness is validated by successfully powering a Humidity, Temperature, and Clock (HTC) sensor using an X-band microwave input, demonstrating its potential for efficient wireless power delivery in drone-based applications.

Keywords: quasi-Yagi antenna; UAV and drone; wide band rectifier, WPT, X-band rectenna

1 INTRODUCTION

Wireless Power Transmission (WPT) has potential applications in solar power satellites and in powering high-altitude platforms such as helicopters, aircraft, UAVs, and drones [1]. In Space Solar Power Satellite systems, solar energy is transmitted to Earth as a microwave or laser beam and converted to DC power, though laser systems have low efficiency despite their low divergence. [2, 3]. In [4], a mmWave WPT system utilizes leaky-wave antennas for passive beam scanning without active phased arrays. A magnetoelectric dipole-based rectenna achieves over 50% RF-to-DC efficiency. In [5], two 2 × 2 polarization-insensitive dual-polarized rectenna arrays using RF and DC power combining strategies are introduced for wireless power transmission. A hybrid coupler ensures equal distribution of horizontal and vertical polarizations, making the rectenna's performance independent of wave polarization. Experimental results validate the polarization insensitivity and highlight the distinct advantages of each combining approach. In [6], an RF power-combined rectenna array operating at 10 GHz was developed for low incident power densities ranging from 0.1 to 100 μW/cm², utilizing circularly polarized patch antenna subarrays. A single-ended Schottky diode rectifier, characterized for varying input powers and loads, is integrated with a 4-to-1 RF power-combining network to improve RF-to-DC conversion efficiency at low power levels. The design employs a three-layer PCB with standard components, enabling straightforward scalability to larger apertures. In [6], a large modular X-band rectenna array operating at 10 GHz, designed for space-to-Earth power beaming with 16 tiles forming a panel over 1 m², was presented. Each rectenna cell uses a 4-antenna subarray feeding a single diode to maximize efficiency at low power densities, achieving over 39% efficiency at 1 W/m² within a 36° × 36° field of view. In [7], a 2-18 GHz broadband rectenna using a Vivaldi antenna, hybrid combiner, and HSMS-2860-based rectifier achieved maximum PCE at 0 mW, though detailed rectifier design for wideband performance was not reported despite the diode's limited operating range. In [8], a low-profile rectenna with a five-element traveling wave antenna array and SMS7630-based rectifier achieved 50% PCE at 10 mW, covering -65° to 65° angles and 11.5-12.5 GHz bandwidth, with testing done at 0.5 m in the near field. In [9], a near-field focused 8×8 array at 5.8 GHz improved PCE from 32.98% to 41.85% by concentrating microwave power on the receiver, enhancing efficiency despite a smaller receiving antenna. Atmospheric attenuation is under 0.06 dB up to space at 10 GHz, and since rectifier PCE drops with frequency, a 10 GHz rectenna is ideal for space-to-Earth microwave power transmission. In [10], an ISM-band microstrip square patch antenna operating at 2450 MHz was designed and simulated using HFSS and CST to evaluate gain, reflection coefficient, and HPBW. The study investigated the effect of adding a co-planar structure, which improved the maximum gain from 0.308 dB to 0.748 dB and reduced HPBW from 55.05° to 49.46°, enhancing directionality without increasing antenna size. Results demonstrated that co-planar structures can effectively boost antenna performance, offering an alternative to traditional size-based gain enhancement methods. In [11], a compact reconfigurable antenna with wide-band and dual-band operation was designed using two closed rings and an ELC structure on a 30 × 31 mm² FR4 substrate. By integrating PIN diodes between the rings and ELC, the antenna achieves switchable frequency bands of 2.4-2.7 GHz and 4.2-4.3 GHz, with bandwidths of 3200 MHz and 98 MHz, respectively. The design maintains over 2 dBi gain across all bands, offering a compact and efficient solution for WiMAX and WLAN applications. In [12], a compact 4 × 4 S-band rectangular patch rectenna array was proposed and experimentally validated for microwave wireless power transmission (MWPT) applications. A cost-effective rectifier using parallel capacitors as filters was developed, offering improved consistency over traditional designs. The rectenna array achieved an output DC power of 117.6 mW/cm³ and a conversion efficiency of 47.6%. A

rectifier and impedance matching circuit were designed and simulated at 900 MHz for wireless power transmission applications. Real-world WPT deployment for drones or satellites requires overcoming challenges in efficiency, alignment, safety, and integration, while ensuring robustness and cost-effectiveness, far beyond the controlled conditions of lab prototypes.

The reviewed studies demonstrate significant advancements in Wireless Power Transmission (WPT) systems using microwave rectennas across various frequencies and configurations. Peak Power Conversion Efficiencies (PCEs) vary widely depending on frequency, input power, rectifier topology, and antenna design. Notably, efficiencies tend to decrease at higher frequencies due to parasitic effects and diode limitations. Around 10 GHz has emerged as an optimal frequency for space-to-Earth power transmission, balancing atmospheric attenuation and rectifier efficiency. Many designs lack full characterization, particularly reflection coefficients and performance at varying input power levels, which are critical for real-world deployment. While RF combining is more effective for fewer antenna elements, DC combining becomes more efficient as the number of antennas increases. Several systems have achieved high PCEs (up to 71.9%), yet practical validations (e.g., powering an LED or near-field transmission) remain limited in scope.

2 ANTENNA DESIGN

Drones impose strict limitations on payload capacity, making large, high-gain antennas impractical due to their weight and bulk, which can negatively impact flight time and stability. To address this, lightweight, compact, and planar antenna designs, such as microstrip patch arrays, can be implemented using low-density substrates like foam or thin Rogers laminates. Efficient power reception over long distances requires high gain, but small antennas inherently have limited aperture and lower gain. This trade-off can be managed by using high-gain array configurations and employing electrically small antenna techniques optimized for the best size-to-gain performance. Additionally, since drones are mobile and frequently change orientation, circularly polarized antennas help reduce polarization mismatch, while omnidirectional designs can offer better tolerance at the expense of gain. Effective wireless power transmission also requires proper impedance matching between the antenna and the nonlinear rectifier, which varies with input power, necessitating a co-designed system with adaptive or broadband matching networks. To balance the trade-offs between gain, size, and beamwidth, a quasi Yagi-Uda antenna is proposed, offering moderate gain, wider beamwidth, and sufficient bandwidth, making it well-suited for small drone-based WPT applications.

The most suitable operating frequency for powering drones using radiative wireless power transmission (WPT) is in the X-band, as it offers an optimal balance between antenna size, beam focus, and rectifier efficiency. At these frequencies, high-gain directional antennas such as quasi Yagi-Uda or patch arrays can be designed compactly, which is essential for integration into lightweight drone platforms. Additionally, atmospheric attenuation at 10 GHz is minimal, ensuring efficient long-distance energy transfer without significant power loss. Unlike lower frequencies (e.g., 2.45 GHz), which require larger antennas, or higher frequencies (e.g., 24-35 GHz), which suffer from diode inefficiencies and atmospheric absorption, the 10 GHz range provides a practical and efficient compromise, supporting focused beam delivery and high power conversion efficiency in mobile airborne WPT applications.

2.1 Antenna Design

The layout of the five-element quasi-Yagi Uda antenna is illustrated in Fig. 1. The antenna is fabricated on a 10 mil thick Rogers RT/duroid 5880 substrate, which features a low dielectric constant ($\varepsilon_r \approx 2.2$) and an ultra-low loss tangent ($\tan\delta \approx 0.0009$), making it highly suitable for drone-based WPT applications. Its thin, lightweight nature minimizes overall antenna mass, critical for drones with tight payload limitations, while ensuring excellent efficiency and minimal signal degradation at X-band frequencies. The substrate's thermal and mechanical stability further ensures reliable in-flight performance, supporting compact and high-gain configurations such as the quasi-Yagi Uda array. The initial design consists of a three-element configuration comprising a driven dipole, a director, and a reflector. On one side of the substrate, one arm of the driven dipole, the director, a line of the parallel strip line, and a microstrip feed are printed. The opposite side hosts the second arm of the driven dipole, oriented oppositely, along with the second line of the parallel strip line and a truncated ground plane, which functions as the reflector. To transition from the antenna's balanced impedance to a standard 50 Ω unbalanced microstrip line, a quarter-wave impedance transformer using a double-sided printed strip (DSPS) line is employed. The driven dipole's initial length is set to half the guided wavelength ($\lambda g/2$) at the center frequency.

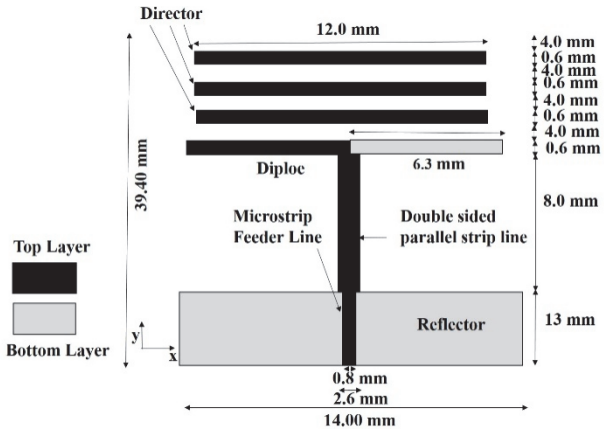

Figure 1 Layout of the quasi- Yagi-Uda antenna

To enhance the antenna's gain, two additional directors are incorporated. The lengths and spacings of the dipole, directors, and ground plane were optimized using the 3D electromagnetic simulation tool Ansys HFSS, with the final dimensions shown in Fig. 1.

2.2 Performance of the Designed Antenna

To validate the antenna design, the antenna was fabricated, with a photograph shown in Fig. 2. Key performance parameters, including the reflection

coefficient and radiation pattern, were measured using a vector network analyzer and tested in an anechoic chamber, as illustrated in Fig. 3a and Fig. 3b, respectively. The simulated and measured reflection coefficients (S_{11} in dB) are presented in Fig. 4, revealing a simulated −10 dB impedance bandwidth of 160 MHz (from 9.96 GHz to 10.12 GHz), while the measured bandwidth is significantly wider at 540 MHz (from 9.70 GHz to 10.24 GHz). The antenna achieved a simulated peak gain of 8.85 dBi at 10 GHz and a measured gain of 8.75 dBi at 9.9 GHz.

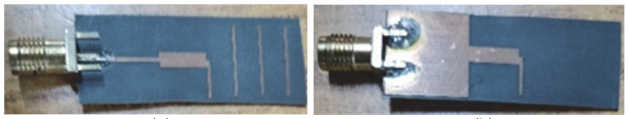

(a) (b)

Figure 2 Photographs of the antenna: (a) Top view (b) Bottom view

(a)

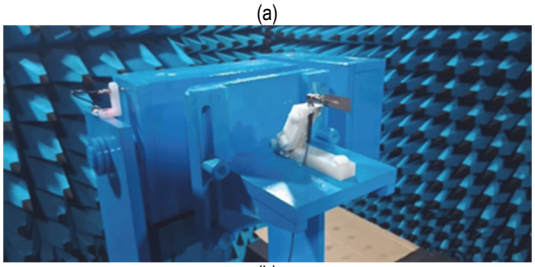

(b)

Figure 3 Measurement setup for measuring antenna parameters: (a) Reflection coefficient; (b) Radiation pattern

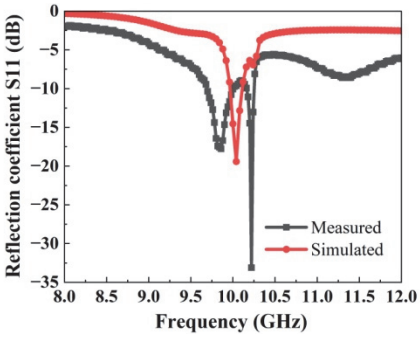

Figure 4 Reflection coefficient of the antenna

The integration of additional directors in the antenna design enhances its radiation characteristics by improving gain. Fig. 5a and Fig. 5b show the radiation patterns in the E-plane and H-plane, with measured half-power beamwidths (HPBW) of 42° and 56°, respectively. The antenna exhibits a front-to-back ratio of 8 dB and low cross-polarization levels in both planes. These results confirm the antenna's effectiveness and suitability for wireless power transfer applications, specifically for powering small drones.

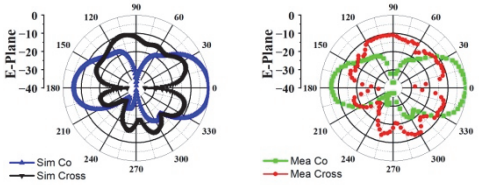

(a)

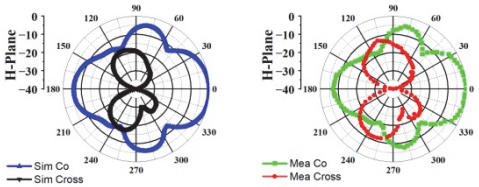

(b)

Figure 5 Simulated and measured radiation pattern: (a) E-plane; (b) H-plane

3 RECTIFIER

The rectifier is essential for converting received RF energy into usable DC voltage and current. High-frequency rectifiers are typically optimized for peak efficiency at a specific input power, center frequency, and load impedance. However, their performance significantly deteriorates outside these operating conditions, mainly due to impedance mismatch between the antenna and rectifier. This issue stems from the non-linear characteristics of the diode, whose input impedance varies with changes in input power, frequency, and load. Consequently, designing an efficient matching network that ensures consistent performance across a range of power levels is a major challenge in rectifier development. In [5], both analytical and experimental studies were conducted on RF and DC combiner rectenna topologies. The RF combiner approach channels RF power from multiple antennas into a single rectifier, making it highly efficient for narrow-beam, point-to-point systems. In contrast, the DC combiner topology assigns individual rectifiers to each antenna, combining the resulting DC outputs in series, parallel, or hybrid configurations, ideal for large-area rectenna arrays. The RF combiner is more effective near the main beam due to concentrated power delivery, while the DC combiner captures power from broader angles due to wider beamwidths of individual elements. Effective wireless power transfer (WPT) requires precise impedance matching between the antenna and rectifier, which is further complicated by the variable nature of input conditions. This underscores the need for a rectifier circuit that performs efficiently at higher power levels in RF combiner systems and at moderate power levels in DC combiner configurations, supported by a matching network capable of adapting to varying conditions. Designing a rectenna system for wireless power transfer poses the challenge of achieving a wide PCE bandwidth to ensure efficient power conversion across varying frequencies, while also maintaining tolerance to impedance mismatches and load variations typical in drones, IoT, and mobile applications, critical for delivering consistent and reliable performance amid environmental changes and interference. Therefore, the aim of this research is to design a rectifier integrated with a matching circuit that addresses these challenges, specifically tailored for wireless power transmission in the X-band.

3.1 Rectifier Design

The rectifier circuit comprises a diode, matching network, low-pass filter, DC pass filter, and load resistor. Both schematic and layout-level simulations are performed using Advanced Design System (ADS) software. The circuit is implemented on 10 mil thick Rogers RT Duroid 5880 substrate, which offers a low dielectric constant of 2.2 and a loss tangent of 0.0009, making it ideal for high-frequency applications. The Avago HSMS-8202 Schottky diode is chosen for rectification due to its suitability for X/Ku-band frequencies. This diode features a low forward voltage drop of 350 mV, a series resistance of 6 Ω, a junction capacitance of 0.18 pF, and a breakdown voltage of 4 V. During operation, the diode generates harmonic signals, which are managed using a low-pass filter at the input and a DC pass filter at the output. The input low-pass filter suppresses the re-radiation of harmonics by the antenna and redirects these harmonic components back to the diode for further rectification, thereby enhancing overall efficiency. At the output, the DC pass filter, composed of three radial stubs, is designed to suppress the first, second, and third harmonics, reduce ripple, and ensure that only the DC component reaches the load. The layout of the DC pass filter is illustrated in Fig. 6. The simulated reflection coefficient (S_{11}) and transmission coefficient (S_{21}) are shown in Fig. 7, demonstrating that the transmission levels for the first, second, and third harmonics are all below −15 dB, indicating effective suppression of these unwanted frequency components.

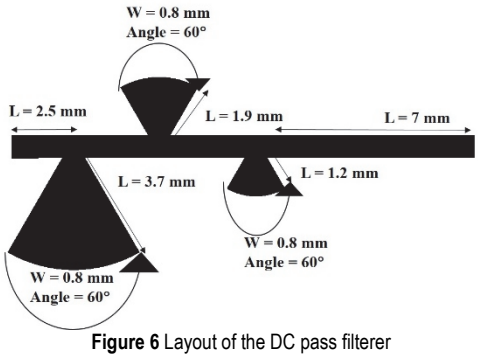

Figure 6 Layout of the DC pass filterer

A fifth-order stepped impedance Chebyshev low-pass filter was designed with a cut-off frequency of 11.5 GHz, targeting 30 dB attenuation at 20 GHz and a passband ripple of 0.2 dB. The layout of the proposed filter is shown in Fig. 8. The simulated reflection and transmission coefficients, presented in Fig. 9, indicate 22 dB attenuation at 20 GHz and confirm the filter's effective performance in both the passband and stopband. A fifth-order Chebyshev filter offers a sharper roll-off than a Butterworth filter, achieving better stopband attenuation near 20 GHz. It maintains acceptable passband ripple, balancing performance and design simplicity. Compared to elliptic filters, it avoids layout complexity while still delivering effective attenuation in high-frequency applications.

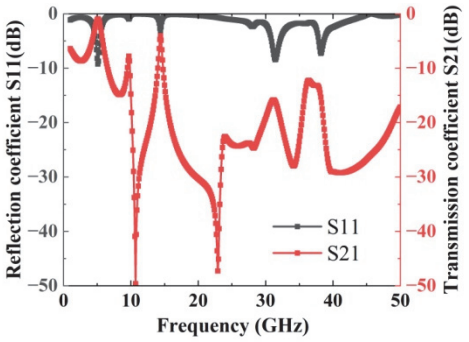

Figure 7 Reflection and transmission coefficients of the DC pass filterer

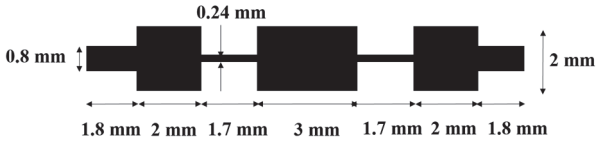

Figure 8 Layout of the stepped impedance low-pass filterer

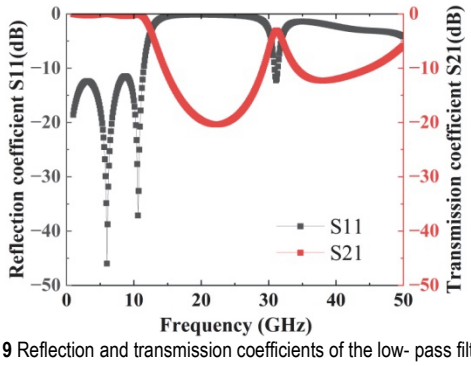

Figure 9 Reflection and transmission coefficients of the low- pass filterer

Figure 10 Layout of the rectifer circuit featuring a two section quarter wave transformer, LPF and DC pass filter

The input impedance of a diode-based rectifier circuit varies with input power level, operating frequency, and load resistance. In this work, the input impedance of the rectifier comprising the diode, DC pass filter, and load resistor was analyzed at 10 GHz and 30 mW input power using Large Signal S-Parameter (LSSP) and Harmonic Balance simulations in ADS software. Since the diode typically presents a complex impedance, impedance matching is essential and is commonly achieved using lumped or distributed matching networks. To address this, a two-section quarter-wave transformer was employed in this design to enhance matching across a range of power levels, frequencies, and load conditions. The layout of the rectifier circuit, including the diode, two-section quarter-wave line, low-pass filter, and DC pass filter, is shown in Fig. 10. Fig. 11a and Fig. 11b compare the simulated reflection coefficient (S_{11}) for single and two-section quarter-wave line matching networks at input power levels of 10 mW and 30 mW, respectively, with a 500 Ω load. The results show that the two-section quarter-wave matching network significantly enhances the impedance bandwidth. Additionally, the matching network introduces a second resonance at 11 GHz frequency for an input power level of 30 mW.

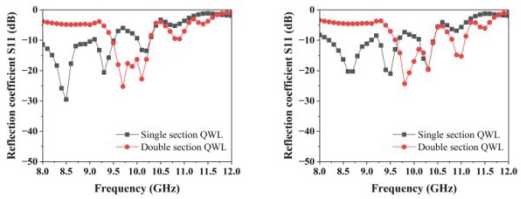

(a) (b)

Figure 11 Simulated reflection coefficient of the rectifer circuit featuring an impedance matching network, LPF and DC pass filter:(a) 10 mW; (b) 30 mW

3.2 Performance of the proposed rectifier design

The layout of the rectifier circuit, comprising a diode, two-section quarter-wave line, low-pass filter, and DC pass filter, as illustrated in Fig. 10, was analyzed for its reflection coefficient and power conversion efficiency (PCE) under various power levels, load resistances, and operating frequencies. The power conversion efficiency is calculated by

$$\eta = \frac{V_L^2}{R_L P_{\text{in}}} \cdot 100 \qquad (1)$$

R_L is load resistance, P_{in} is input microwave power and V_L is output dc voltage of the load.

The simulated reflection coefficients for power levels ranging from 1 mW to 20 mW and from 30 mW to 100 mW at a 500 Ω load resistor are presented in Fig. 12a and Fig. 12b, respectively. At a 500 Ω load, the rectifier circuit achieves a −10 dB impedance bandwidth of 500 MHz at 10 mW and 20 mW input power levels, and 700 MHz at 30 mW, 40 mW, and 50 mW. The corresponding simulated PCE values for the same power ranges and load resistance are shown in Fig. 13a and Fig. 13b. Fig. 14a and Fig. 14b further show the simulated PCE across different frequencies and load resistances. A PCE greater than 40% is achieved across a 750 MHz bandwidth (from 9.5 GHz to 10.25 GHz) for power levels of 5 mW, 10 mW, and 20 mW, and across a 1500 MHz bandwidth (from 9.5 GHz to 11.0 GHz) for power levels of 30 mW, 40 mW, and 50 mW, all at a 500 Ω load. The rectifier circuit achieves a maximum PCE of 64% at a frequency of 9.75 GHz and an input power of 30 mW. Additionally, a PCE exceeding 40% is observed across a wide range of load resistances (200 Ω to 1000 Ω) for power levels of 5 mW, 10 mW, 20 mW, and 30 mW. With a maximum PCE of 64% at 9.75 GHz, the rectifier is well-suited for low-power wireless applications. It can efficiently power auxiliary systems in small drones (20-100 mW), IoT sensor nodes (10-50 mW), RFID or smart tags (5-30 mW), and remote environmental sensors (15-40 mW). To validate the design, the rectifier circuit was fabricated. A photograph of the fabricated board is shown in Fig. 15. Fig. 16a and Fig. 16b display the measurement setups for the reflection coefficient using a network analyzer and for PCE using a microwave signal generator and a multimeter, respectively.

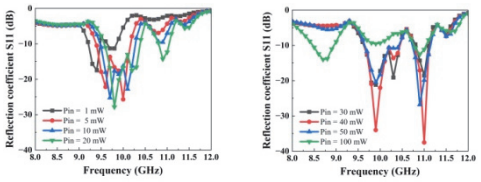

(a) (b)

Figure 12 Simulated reflection coefficient of the rectifer circuit at different power levels: (a) 1 mW to 20 mW; (b) 30 mW to 100 mW

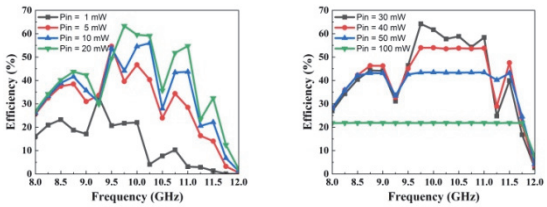

(a) (b)

Figure 13 Simulated efficiency versus frequency of the rectifer circuit at different power levels: (a) 1 mW to 20 mW; (b) 30 mW to 100 mW

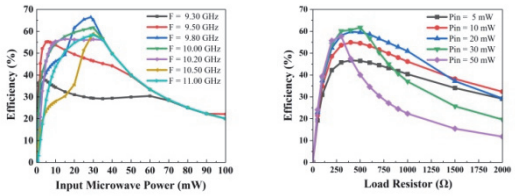

(a) (b)

Figure 14 Simulated efficiency versus frequency of the rectifer circuit : (a) different frequencies; (b) different load resistors

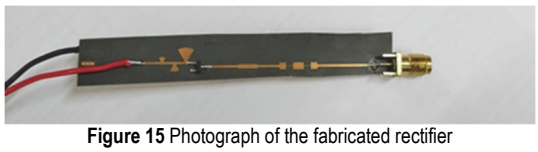

Figure 15 Photograph of the fabricated rectifier

(a) (b)

Figure 16 Photograph of the rectifier board under measurement: (a) Reflection coefficient; (b) Efficiency

Fig. 17 and Fig. 18 present the measured and simulated reflection coefficients for load resistors of 462 Ω and 982 Ω, respectively. The results indicate that the impedance bandwidth is greater for the 462 Ω load. Fig. 19a and Fig. 19b show the measured power conversion efficiency (PCE) at different input power levels for load resistors of 462 Ω and 982 Ω, respectively, while Fig. 20a and Fig. 20b illustrate the measured PCE across different frequencies for the same load values. For the 462 Ω load resistor, the rectifier circuit achieves a bandwidth of 1.75 GHz where the PCE remains above 40% over an input power range of 20 mW to 50 mW. Additionally, it maintains a PCE of at least 50% over a 0.75 GHz bandwidth within the power range of 30 mW to 50 mW. In comparison, the rectifier circuit with a 982 Ω load resistor delivers a 1.50 GHz bandwidth with PCE exceeding 40% across the 20 mW to 50 mW input power range. Lower load resistance (462 Ω) results in a wider impedance bandwidth and higher power

conversion efficiency (PCE) over a broader frequency and input power range compared to a higher load resistance (982 Ω)

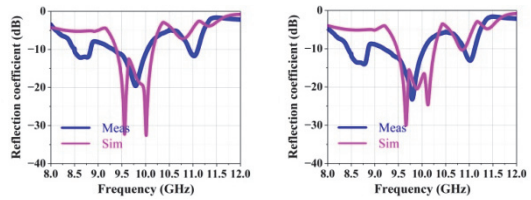

Figure 17 Measured reflection coefficient of the rectifier for a load resistor of 462 Ω: (a) P_{in} = 5 mW; (b) P_{in} = 10 mW.

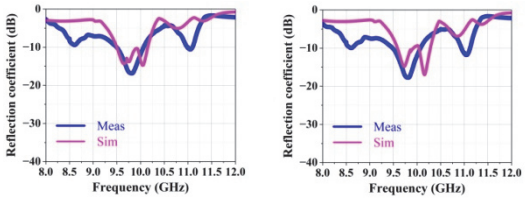

Figure 18 Measured reflection coefficient of the rectifier for a load resistor of 982 Ω: (a) P_{in} = 5 mW; (b) P_{in} = 10 mW

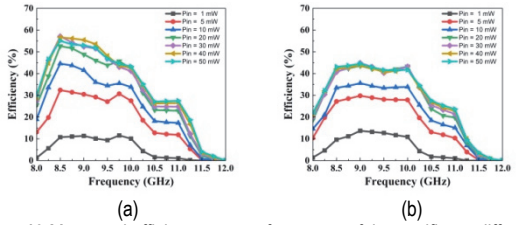

Figure 19 Measured efficiency versus frequency of the rectifier at different power levels: (a) R_L = 462Ω; (b) R_L = 982 Ω

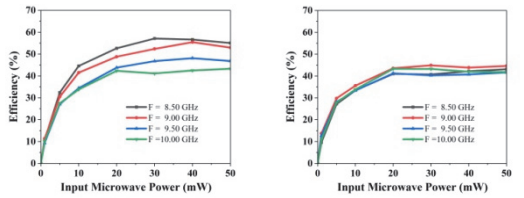

Figure 20 Measured efficiency versus input power of the rectifier at different frequencies:(a) R_L = 462Ω; (b) R_L = 982 Ω

The performance of the fabricated rectenna for wireless power transmission was evaluated using an X-band microwave setup in an indoor environment, as shown in Fig. 21.

Figure 21 Photograph of experimental set-up for powering the sensor using the proposed rectenna

The rectenna was positioned 15 centimeters away from the transmitting horn antenna, placing it within the near-field testing range. The RF input signal, generated by a microwave source, was used to power a Humidity, Temperature, and Clock (HTC) sensor via the fabricated rectenna circuit. These results demonstrate the potential of the proposed rectenna for effective wireless power transmission.

4 DISCUSSION OF RESULTS

One of the main requirements in wireless power transfer (WPT) systems is to maximize DC output power. At higher input power levels, the PCE of rectifier circuits typically decreases, resulting in reduced DC power. Therefore, improving PCE at higher power levels is crucial. Another key design goal is to increase operational bandwidth, enabling the rectifier to support multi-band energy harvesting and function effectively across different frequency bands using the same circuit. The performance metrics of the fabricated antenna and the rectifier are summarized in Tab. 1 and Tab. 2 respectively. The performance of the proposed rectifier design is compared with the previous researches in the Tab. 3. In Ref. [7], maximum PCE values of 38% and 18% are achieved at 10 mW and 31.6 mW, respectively, for 10 GHz operation. However, a PCE of 70% is reported at 1 mW, attributed to the HSMS-2862 diode used, which operates efficiently at lower power levels and has an effective frequency range up to 5.8 GHz. In Ref. [8], a maximum PCE of 50% is achieved at 10 mW, and nearly the same PCE is maintained across the frequency range of 11.5 GHz to 12.6 GHz, using a single-stub matching network for optimal power transfer. For instance, in [12], rectifiers utilizing surface-mount capacitors and serpentine microstrip filters achieved rectification efficiencies exceeding 50% at high input power levels (630-2000 mW), with peak efficiencies of 57.0% and 57.6%, respectively. In [6], an open stub matching network achieved 40% PCE at 10 mW and 10 GHz. However, these results were limited to narrow frequency ranges.

Table 1 Performance metrics of the fabricated antenna

Parameters	Values
−10 dB impedance bandwidth	540 MHz (9.70 GHz-10.24 GHz)
Antenna Gain	8.75 dBi
HPBW in H-plane	56°
HPBW in E-plane	42°
Cross Polarization	−15 dB
FBR	8 dB
Size	4 × 1.7 cm

Table 2 Performance metrics of the fabricated rectifier

Input Power / mW	Maxiumu PCE / %		Bandwidth / GHz for PCE ≥ 40%	
	462 Ω	982 Ω	462 Ω	982 Ω
1	11.6	13.7	-	-
5	32.4	29.8	-	-
10	44.6	35.6	0.75	
20	52.6	43.6	1.75	1.50
30	57.1	44.9	1.75	1.50
40	56.6	43.8	1.75	1.50
50	55.1	44.6	1.75	1.50

In contrast, the proposed rectifier is optimized for higher input power levels (20-50 mW), maintaining a PCE above 40% across this entire range and peaking at 53%, 57%, 57%, and 55% for 20 mW, 30 mW, 40 mW, and 50 mW, respectively. It also exhibits superior frequency performance, achieving over 50% PCE across 8.50-9.25

GHz for 30-50 mW and over 40% PCE across a broader 8.25-10.00 GHz range for 20-50 mW input power. Compared to Refs. [6] and [7], the proposed design offers significantly higher efficiency at elevated power levels and competitive bandwidth. While Ref. [8] achieves ~ 50% PCE over a 1 GHz bandwidth at 10 mW, the proposed design attains 0.75 GHz bandwidth for > 50% PCE at higher power levels and 1.75 GHz for > 40% PCE. Overall, the proposed rectifier demonstrates enhanced performance in terms of PCE and bandwidth, meeting key WPT requirements such as high DC output at elevated power levels and multi-band operation without significantly increasing circuit size.

Table 3 Performance comparison of the rectifier against related works

Ref. No.	Frequency / GHz	Power Level / mW	PCE / %	Bandwidth for PCE	Size / mm2
[6]	10	10	40	NA	NA
[7]	10	10 15	38 18	X-band for PCE < 40%	80 × 25
[8]	12	10	50	1 GHz for PCE ≅ 50%	100 × 30
[12]	2.45	32	57.6	NA	27 × 28
This work	8.5	14.8 17	57 55	1.75 GHz for PCE > 40%	80 × 10

Enhancing the beamwidth of microstrip patch antennas is critical for applications requiring wide-angle coverage, such as wireless sensing and communication systems. Traditional techniques used to increase beamwidth in patch antennas include stacked patch configurations, low-dielectric or thin substrates, modified patch geometries, multiple feeding points, parasitic elements, and defected ground structures. While these methods can effectively broaden the radiation pattern, they often come at the cost of increased antenna complexity, larger size, or reduced gain. For instance, in [7], five microstrip line traveling wave antennas (TWAs) were designed to collectively provide 120° of angular coverage. Each antenna in the array was tailored to cover a 30° sector corresponding to specific beam directions at −60°, −30°, 0°, 30°, and 60°, achieving a maximum gain of 12 dBi across the 11.5 GHz to 12.5 GHz frequency band. The overall size of the five-antenna array is 10 × 10 cm. In the present work, a compact quasi-Yagi antenna array is proposed, which achieves a good balance between beamwidth and gain while significantly reducing physical dimensions. The designed antenna exhibits 3 dB beamwidths of 42° in the E-plane and 56° in the H-plane, with an overall size of just 4 × 1.7 cm and a measured gain of 8.75 dBi. Compared to the designs in [7], the proposed quasi-Yagi antenna demonstrates a more compact footprint and simpler structure, making it suitable for space-constrained applications. While the gain is slightly lower than that of the TWA design, the wider beamwidth and reduced complexity present a favorable trade-off. These results confirm that the proposed design effectively balances beamwidth, gain, size, and design simplicity, making it a strong candidate for integration in modern wide-coverage antenna systems.

5 CONCLUSION

The proposed rectifier design exhibits high performance with peak PCE values between 53% and 57% across input power levels of 30-50 mW, maintaining over 50% PCE within a 0.75 GHz bandwidth and exceeding 40% across a wider 1.75 GHz range. This represents a significant improvement over previous works, particularly at higher power levels. The integrated quasi-Yagi antenna further enhances the system's efficiency, offering wide beamwidths (42° E-plane, 56° H-plane), moderate gain (8.75 dBi), and a compact form factor, effectively balancing beamwidth, gain, size, and design complexity. The rectenna's capability was successfully demonstrated by powering a Humidity, Temperature, and Clock (HTC) sensor using an X-band microwave input, confirming its suitability for efficient wireless power transmission applications.

6 REFERENCES

[1] Surender, D., Khan, T., Talukdar, F. A., & Antar, Y. M. (2021). Rectenna design and development strategies for wireless applications: A review. *IEEE Antennas and Propagation Magazine*, *64*(5), 16-29. https://doi.org/10.1109/MAP.2021.3099722

[2] Shinohara, N. (2020). Trends in wireless power transfer: WPT technology for energy harvesting, millimeter-wave/THz rectennas, MIMO-WPT, and advances in near-field WPT applications. *IEEE Microwave Magazine*, *22*(1), 46-59. https://doi.org/10.1109/MMM.2020.3027935

[3] Nosrati, M., Rezaei, P., Danaie, M., & Khalilpour, J. (2025). Broadband compact rectenna system using a Wilkinson power divider to harvest microwave energy. *Scientific Reports*, *15*(1). https://doi.org/10.1038/s41598-025-02555-1

[4] Song, C., Wang, L., Lu, P., Zhang, C., Chen, Z., Zheng, X., He, Y., Goussetis, G., Vandenbosch, G. A., & Huang, Y. (2023). Highly efficient wideband mmWave rectennas for wireless power transfer system with low-cost multinode tracking capability. *IEEE Transactions on Antennas and Propagation*, *71*(11), 8773-8787. https://doi.org/10.1109/TAP.2023.3313182

[5] Sun, H., He, H., & Huang, J. (2020). Polarization-insensitive rectenna arrays with different power combining strategies. *IEEE Antennas and Wireless Propagation Letters*, *19*(3), 492-496. https://doi.org/10.1109/LAWP.2020.2968616

[6] Tierney, B. B., Rodenbeck, C. T., Parent, M. G., & Self, A. P. (2021). Scalable, high-sensitivity X-band rectenna array for the demonstration of space-to-earth power beaming. *IEEE Access*, *9*, 27897-27907. https://doi.org/10.1109/ACCESS.2021.3057020

[7] Nosrati, M., Rezaei, P., Danaie, M., & Khalilpour, J. (2025). A broadband integrated rectenna for microwave radio energy harvesting using an integrated hybrid sandwich power divider. *e-Prime-Advances in Electrical Engineering, Electronics and Energy*, *11*, 100891. https://doi.org/10.1016/j.prime.2024.100891

[8] Ha, T. D., Nie, X., Bağcı, H., Erricolo, D., & Chen, P. Y. (2024). A low-profile, wide-angle, and bandwidth enhanced rectenna for radiative energy harvesting in the 12 GHz band. *IEEE Antennas and Wireless Propagation Letters*, *23*(11), 3807-3811. https://doi.org/10.1109/LAWP.2024.3387925

[9] Yi, X., Chen, X., Zhou, L., Hao, S., Zhang, B., & Duan, X. (2019). A microwave power transmission experiment based

on the near-field focused transmitter. *IEEE Antennas and Wireless Propagation Letters*, *18*(6), 1105-1108. https://doi.org/10.1109/LAWP.2019.2910200

[10] Armagan, O. & Kahriman, M. (2022). The effect of the co-planar structure on HPBW and the directional gain at the square patch antenna around ISM 2450 MHz. *Tehnicki vjesnik-Technical gazette*, *29*(4), 1120-1125. https://doi.org/10.17559/TV-20190423010908

[11] Jansirani, G. & Gandhi Raj, R. (2024). Miniaturised wide and dual band reconfigurable antenna on-demand for portable wireless devices. *Tehnicki vjesnik-Technical gazette*, *31*(6), 2022-2027. https://doi.org/10.17559/TV-20240122001282

[12] Huang, D., Li, J., Du, Z., Liu, C., He, Z., & Zhang, J. (2024). A compact and high-power rectenna array for wireless power transmission applications. *Energies*, *17*(23), 6008. https://doi.org/10.3390/en17236008

Contact information:

V. GANESH, Assistant Professor
(Corresponding Author)
Department of Electronics and Communication Engineering,
Sri Ramakrishna Institute of Technology, Coimbatoe, Tamil Nadu, India
E-mail: ganeshperumal.ece@outlook.com

H. MANGALAM, Professor
Department of Electronics and Communication Engineering,
Sri Ramakrishna Engineering College, Coimbatore, Tamil Nadu, India
E-mail: hmangalam2@gmail.com